Low-field magnetization of magnetic random-mixture graphite intercalation compounds

Itsuko S. Suzuki and Masatsugu Suzuki
Department of Physics, State University of New York at Binghamton, Binghamton, New York 13902-6000

Yusei Maruyama
Institute for Molecular Science, Myodaiji, Okazaki 444, Japan
(Received 2 June 1993; revised manuscript received 2 August 1993)

We have measured the temperature dependence of low-field SQUID magnetization for random-mixture graphite intercalation compounds (GICs), stage-2 $Co_cNi_{1-c}Cl_2$ GICs, stage-2 $Ni_cMn_{1-c}Cl_2$ GICs, and stage-2 $Co_cMn_{1-c}Cl_2$ GICs. For stage-2 $Co_cNi_{1-c}Cl_2$ GICs ($0 \le c \le 1$), stage-2 $Ni_cMn_{1-c}Cl_2$ GICs ($0.8 \le c \le 1$), and stage-2 $Co_cMn_{1-c}Cl_2$ GICs ($0.9 \le c \le 1$) where ferromagnetic intraplanar exchange interactions are dominant within each island in the magnetic intercalate layers, the zero-field-cooled (ZFC) magnetization of these compounds deviates downward from the field-cooled (FC) magnetization below a critical temperature T_c, and shows a broad peak at a temperature $T_{max}(<T_c)$. This irreversible effect of magnetization indicates that a cluster glass phase appears below T_c. The ferromagnetic spin order is established within each island, forming a ferromagnetic cluster. The spin directions of these ferromagnetic clusters are frozen because of frustrated interisland interactions consisting of both the dipole-dipole interaction between ferromagnetic clusters and antiferromagnetic interplanar exchange interaction between different intercalate layers. The broad peak of ZFC arises as a result of a competition between thermal energy and these frustrated interisland interactions.

I. INTRODUCTION

Magnetic random-mixture graphite intercalation compounds (RMGICs) such as $Co_cNi_{1-c}CI_2$ GICs (Refs. 1–3), $Ni_cMn_{1-c}Cl_2$ GICs (Ref. 4), $Co_cMn_{1-c}Cl_2$ GICs (Refs. 5 and 6), and $Co_cMg_{1-c}Cl_2$ GICs (Refs. 7 and 8) are new types of GICs where the intercalate layers are formed of a random mixture of two kinds of intercalants such as $CoCl_2$, $NiCl_2$, $MnCl_2$, and $MgCl_2$. These magnetic RMGICs form a class of materials whose dimension can be systematically controlled by the number of graphite layers between adjacent intercalate layers, i.e., the stage number. Because of recent progress in sample preparation these magnetic RMGICs provide model systems for studying the magnetic phase transitions of two-dimensional (2D) random spin systems where various kinds of spin frustration effect occur as a result of the competing intraplanar ferromagnetic and antiferromagnetic interactions, and the competing spin anisotropy between Ising, *XY* and Heisenberg symmetry. The intercalate layer of these magnetic RMGICs has a unique 2D complex lattice formed of small islands whose diameter is on the order of 500 Å. The peripheral chlorine ions at the island boundary provide acceptor sites for charges transferred from the graphite layer to the intercalate layer. The growth of spin correlation length within intercalate layers may be limited by the existence of small islands. The 2D ferromagnetic order thus established within each island is denoted as a ferromagnetic cluster.

In this paper we have undertaken an extensive study on the magnetic phase transitions of stage-2 $Co_cNi_{1-c}Cl_2$ GICs, stage-2 $Ni_cMn_{1-c}Cl_2$ GICs, and stage-2 $Co_cMn_{1-c}Cl_2$ GICs. We will present our experimental results of SQUID (superconducting quantum interference device) magnetization measurement on these compounds: the temperature dependence of zero-field cooled (ZFC) magnetization and field-cooled (FC) magnetization. We will show that the ZFC magnetization of stage-2 $Co_cNi_{1-c}Cl_2$ GICs with $0 \le c \le 1$, stage-2 $Ni_cMn_{1-c}Cl_2$ GICs with $0.8 \le c \le 1$, and stage-2 $Co_cMn_{1-c}Cl_2$ GICs with $0.9 \le c \le 1$ deviates downward from the FC magnetization below a critical temperature T_c and shows a broad peak at a temperature T_{max}. We will also show that the ZFC magnetization of stage-2 $Ni_cMn_{1-c}Cl_2$ GICs ($0.7 \le c < 0.8$) and stage-2 $Co_cMn_{1-c}Cl_2$ GICs ($0.8 \le c < 0.9$) is characterized by the irreversible effect below T_c and the absence of any broad peak. The model of magnetic phase transition in these compounds will be presented to explain the temperature dependence of the ZFC and FC magnetization.

The format of this paper is as follows. In Sec. II we will give a brief summary of the magnetic properties of magnetic binary GICs such as stage-2 $CoCl_2$ GIC, stage-2 $NiCl_2$ GIC, and stage-2 $MnCl_2$ GIC, and magnetic RMGICs such as stage-2 $Co_cNi_{1-c}Cl_2$ GICs, stage-2 $Ni_cMn_{1-c}Cl_2$ GICs, and stage-2 $Co_cMn_{1-c}Cl_2$ GICs. In Sec. III we describe the experimental procedure of SQUID magnetization and electron microprobe measurements. In Sec. IV we present our experimental results of ZFC and FC magnetization for stage-2 $Co_cNi_{1-c}Cl_2$ GICs, stage-2 $Ni_cMn_{1-c}Cl_2$ GICs, and stage-2 $Co_cMn_{1-c}Cl_2$ GICs. Discussions of experimental results are given in Sec. V.

II. BACKGROUND

A. Spin Hamiltonian (Refs. 9–12)

The stage-2 $CoCl_2$ GIC approximates to a quasi 2D Heisenberg ferromagnet (fictitious spin $S=\frac{1}{2}$) with large XY anisotropy. The spin Hamiltonian for Co^{2+} ions is described by the intraplanar exchange interaction [J(Co-Co)=7.75 K], the anisotropic exchange interaction J_A [J_A/J(Co-Co)=0.48], and the antiferromagnetic interplanar exchange interaction J'[$|J'|/J$(Co-Co)$\approx 10^{-4}$]. The effective magnetic moment of the Co^{2+} ion is given by $P_{\text{eff}}(\text{Co})=g(\text{Co})[S(S+1)]^{1/2}=5.54\mu_B$ for the g value g(Co)=6.40. The stage-2 $NiCl_2$ GIC approximates to a quasi 2D Heisenberg ferromagnet ($S=1$) with small XY anisotropy. The spin Hamiltonian of Ni^{2+} ions is described by the ferromagnetic intraplanar exchange interaction J(Ni-Ni)=8.75 K, the single-ion anisotropy parameter D(Ni)=0.80 K, and the very weak antiferromagnetic interplanar interaction J'[$|J'|/J$(Ni-Ni)$\approx 10^{-3}$]. The effective magnetic moment of Ni^{2+} ions is given by $P_{\text{eff}}(\text{Ni})=g(\text{Ni})[S(S+1)]^{1/2}=3.29\mu_B$ for g(Ni)=2.33. The stage-2 $MnCl_2$ GIC approximates to a quasi 2D Heisenberg antiferromagnet (spin $S=\frac{5}{2}$) with XY anisotropy. The spin Hamiltonian of Mn^{2+} ions is described by the antiferromagnetic intraplanar interaction J(Mn-Mn)$=-0.2$ K and the single-ion anisotropy parameter D(Mn)=0.97 K. The effective magnetic moment of the Mn^{2+} ion is given by $P_{\text{eff}}(\text{Mn})=g(\text{Mn})[S(S+1)]^{1/2}=6.04\mu_B$ for g(Mn) =2.04.

B. Magnetic properties of magnetic RMGICS

The stage-2 $Co_cNi_{1-c}Cl_2$ GICs magnetically behave like a quasi 2D Heisenberg ferromagnet with XY spin anisotropy.[1–3] The spin symmetry continuously changes from Heisenberg-like at $c=0$ to XY-like at $c=1$. The Co^{2+} and Ni^{2+} spins are distributed randomly on triangular lattice sites of each intercalate layer. The intraplanar exchange interaction J(Co-Ni) between the different spins is larger than that between like spins, J(Co-Co) or J(Ni-Ni): J(Co-Ni) $=1.2[J(\text{Co-Co})J(\text{Ni-Ni})]^{1/2}=9.88$ K. The stage-2 $Ni_cMn_{1-c}Cl_2$ GICs are 2D random-spin systems with competing ferromagnetic and antiferromagnetic exchange interactions.[4] The Curie-Weiss temperature increases monotonically with increasing Ni concentration. Its sign changes from negative to positive around $c\approx 0.22$. The exchange interaction between Ni and Mn spins is ferromagnetic and is described by J(Ni-Mn)$=1.09[J(\text{Ni-Ni})|J(\text{Mn-Mn})|]^{1/2}=1.44$ K. In spite of ferromagnetic J(Ni-Mn), the ferromagnetic long-range order of Ni^{2+} disappears below $c\approx 0.6$. The stage-2 $Co_cMn_{1-c}Cl_2$ GICs are 2D random-spin systems with competing ferromagnetic and antiferromagnetic exchange interactions.[5,6] The Curie-Weiss temperature increases monotonically with increasing Co concentration. Its sign changes from negative to positive around $c\approx 0.2$. The exchange interaction between Co and Mn spins is ferromagnetic and described by J(Co-Mn) $=1.2[J(\text{Co-Co})|J(\text{Mn-Mn})|]^{1/2}=1.49$ K.

III. EXPERIMENTAL PROCEDURE

The dehydration of ACl_2 and BCl_2 (A,B =Co,Ni,Mn) was done at 400 °C in the presence of HCl gas at a pressure of one atmosphere. Single crystals of $A_cB_{1-c}Cl_2$ over the entire range of A concentrations were grown by using the Bridgeman method: a mixture of dehydrated ACl_2 and BCl_2 with the nominal weight composition was heated in quartz sealed in vacuum at 990 °C. The stage-2 $A_cB_{1-c}Cl_2$ GICs were synthesized by intercalating single crystal $A_cB_{1-c}Cl_2$ into single-crystal kish graphite in a chlorine gas atmosphere at a pressure of 740 Torr. The reaction was continued at 520–540 °C for 20 days. The stage of these GIC samples was confirmed to be well-defined stage 2 from (00L) x-ray scattering experiments by using a Huber double-circle diffractometer with a Siemens 2.0 kW x-ray generator.

The actual concentration of stage-2 $A_cB_{1-c}Cl_2$ GIC samples may be different from the concentration of pristine compounds $A_cB_{1-c}Cl_2$ used as intercalants. We determined the concentration of RMGIC samples used in the present work by electron microprobe measurement. The measurement was carried out by using a scanning electron microscope (Model Hitachi S-450). The electrons having a kinetic energy of 20 keV penetrate the sample to a depth of the order of 2 μm, spreading out a similar distance. The quoted concentration is the average value of measurements over several different points of the sample. Figure 1 shows the relationship between the bulk concentration (c_b) of intercalant and the concentration (c_e) determined from the electron microprobe measurements for stage-2 $Ni_cMn_{1-c}Cl_2$ GICs. The data of c_e vs

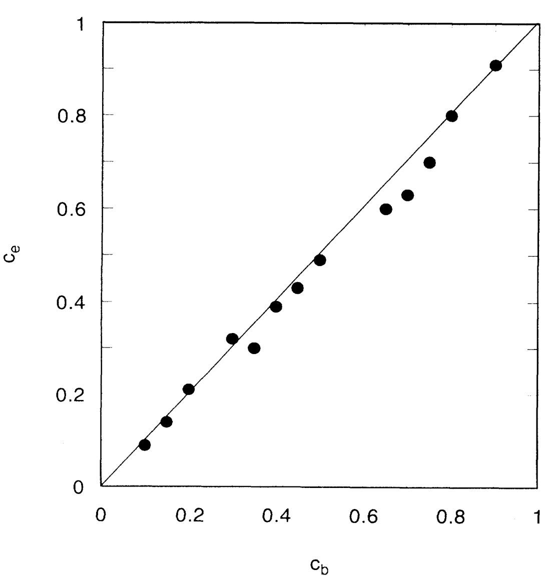

FIG. 1. Relationship between bulk concentration (c_b) of intercalants and concentration (c_e) of their GICs determined from the electron microprobe measurements for stage-2 $Ni_cMn_{1-c}Cl_2$ GICs. The solid line denotes the straight line of $c_e=c_b$.

c_b in stage-2 $Ni_cMn_{1-c}Cl_2$ GICs agree with a straight line of $c_e=c_b$ in the entire concentration of c_b. The data of c_e vs c_b in stage-2 $Co_cNi_{1-c}Cl_2$ GICs and stage-2 $Co_cMn_{1-c}Cl_2$ GICs fall on a straight line in the range of $0<c_b\leq 0.4$ and $0.7\leq c_b<1$, but they deviate from a straight line of $c_e=c_b$ in the range of $0.4<c_b<0.7$. The cause of such a deviation may lie in the limited energy resolution of electron microprobe analysis. A large peak of the NiK_α line at 7.472 keV and a small peak of the CoK_β line at 7.649 keV are superimposed for the stage-2 $Co_cNi_{1-c}Cl_2$ GICs. A small peak of the MnK_β line at 6.492 keV and a large peak of the CoK_α line at 6.925 keV are superimposed for stage-2 $Co_cMn_{1-c}Cl_2$ GICs. Experimentally it is a little difficult to separate each contribution from the measured intensities. Therefore this deviation does not imply that c_e is not equal to c_b in the intermediate Co concentration. Hereafter we assume that the actual concentration c is the same as the concentration of the pristine compounds used as intercalant.

The highly sensitive measurements of magnetization were carried out with a SQUID magnetometer (Model VTS-905 SQUID system, manufactured by S. H. E. Corporation). The measurements were performed in three steps. A schematic (H,T) diagram for the process of measurements are shown in Fig. 2. (i) A sample having a weight of 4–7 mg was first cooled to a temperature T_1 from 300 K in five minutes in the absence of external magnetic field: $T_1=2$ K for stage-2 $Co_cMn_{1-c}Cl_2$ GICs, and $T_1=4.2$ K for stage-2 $Co_cNi_{1-c}Cl_2$ GICs and stage-2 $Ni_cMn_{1-c}Cl_2$ GICs. A field of 1 Oe was then applied along any direction perpendicular to the c-axis, and held constant while the measurements were made from T_1 to T_2. (ii) The temperature dependence of zero-field cooled (ZFC) magnetization, M_{ZFC}, was measured while increasing temperature from T_1 to T_2: $T_2=10$ K for stage 2 $Co_cMn_{1-c}Cl_2$ GICs, and $T_2=30$ K for stage 2 $Co_cNi_{1-c}Cl_2$ GICs and stage-2 $Ni_cMn_{1-c}Cl_2$ GICs. (iii) The sample was again cooled in the field of 1 Oe and the temperature dependence of field-cooled (FC) magnetization, M_{FC}, was measured while decreasing temperature from T_2 to T_1.

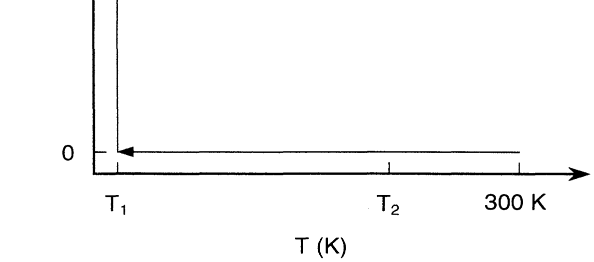

FIG. 2. Schematic (H,T) diagram for the FC and ZFC magnetization measurements.

IV. RESULTS

We have measured the temperature dependence of SQUID magnetization M_{ZFC} and M_{FC} for stage-2 $Co_cNi_{1-c}Cl_2$ GICs with $c=1$, 0.85, 0.65, 0.52, 0.4, 0.25, 0.19, 0.1, and $c=0$, where M_{ZFC} and M_{FC} have been defined in Sec. III. The magnetic field of 1 Oe was applied along any direction perpendicular to the c axis. Typical examples of temperature dependence of M_{ZFC}, M_{FC} and the difference δ $(=M_{FC}-M_{ZFC})$ for stage-2 $Co_cNi_{1-c}Cl_2$ GICs are shown in Fig. 3. For each Co concentration M_{ZFC} shows a broad peak at a temperature denoted by T_{max}. The value of M_{ZFC} at 5 K may depend weakly on the rate of cooling samples from 300 to 5 K in the absence of external magnetic field. The value of T_{max} is independent of the cooling rate. The magnetization M_{ZFC} coincides with M_{FC} at sufficiently high temperatures and begins to deviate downward from M_{FC} at a critical temperature T_c. This irreversible effect of magnetization is considered to be one of the most important features in typical spin glasses. Note that the difference δ monotonically increases with decreasing temperature for any Co concentration, and does not show any anomaly around T_{max}. The magnetization M_{FC} rapidly increases with decreasing temperature below T_c like a spontaneous magnetization of the usual ferromagnet. The value of M_{FC} at 5 K measured in units of emu/av mol is almost independent of Co concentration ($\approx$600 emu/av mol) except for $c=0$. The values of T_c and T_{max} for each Co concentration are derived from the temperature variation of δ and M_{ZFC}, respectively: $T_c=19.4$ K and $T_{max}=17.8$ K for $c=0$, $T_c=17.9$ K and $T_{max}=12.7$ K for $c=0.1$, $T_c=13.0$ K and $T_{max}=9.7$ K for $c=0.4$, and $T_c=9.5$ K and $T_{max}=7.8$ K for $c=1.0$. Figure 4 shows the Co concentration dependence of T_{max} and T_c for the stage-2 $Co_cNi_{1-c}Cl_2$ GICs. The values of T_{max} and T_c monotonically decrease as the Co concentration increases. However, the ratio ρ $(=T_c/T_{max})$ is not a simple function of Co concentration: $\rho=1.09$ at $c=0$, $\rho=1.41$ at $c=0.1$, $\rho=1.34$ at $c=0.4$ and $\rho=1.2$ at $c=1$. The magnetic phase diagram of T_c vs c agrees well with that obtained from the dc and ac magnetic susceptibility measurements.[2,3] The stage-2 $Co_cNi_{1-c}Cl_2$ GICs behave magnetically like a quasi 2D Heisenberg ferromagnet with XY spin anisotropy. The spin symmetry continuously changes from Heisenberg-like at $c=0$ to XY-like at $c=1$. The drastic decrease of T_c with the increase of c around $c=0$ is due to the change of spin symmetry from Heisenberg-like to XY-like.

We have measured the temperature dependence of M_{ZFC} and M_{FC} of stage-2 $Ni_cMn_{1-c}Cl_2$ GICs with $c=1$, 0.9, 0.8, 0.75, 0.7, 0.65, and $c=0.6$. Typical examples of temperature variation in M_{ZFC} and M_{FC} for stage-2 $Ni_cMn_{1-c}Cl_2$ GICs are shown in Fig. 5. We find that the

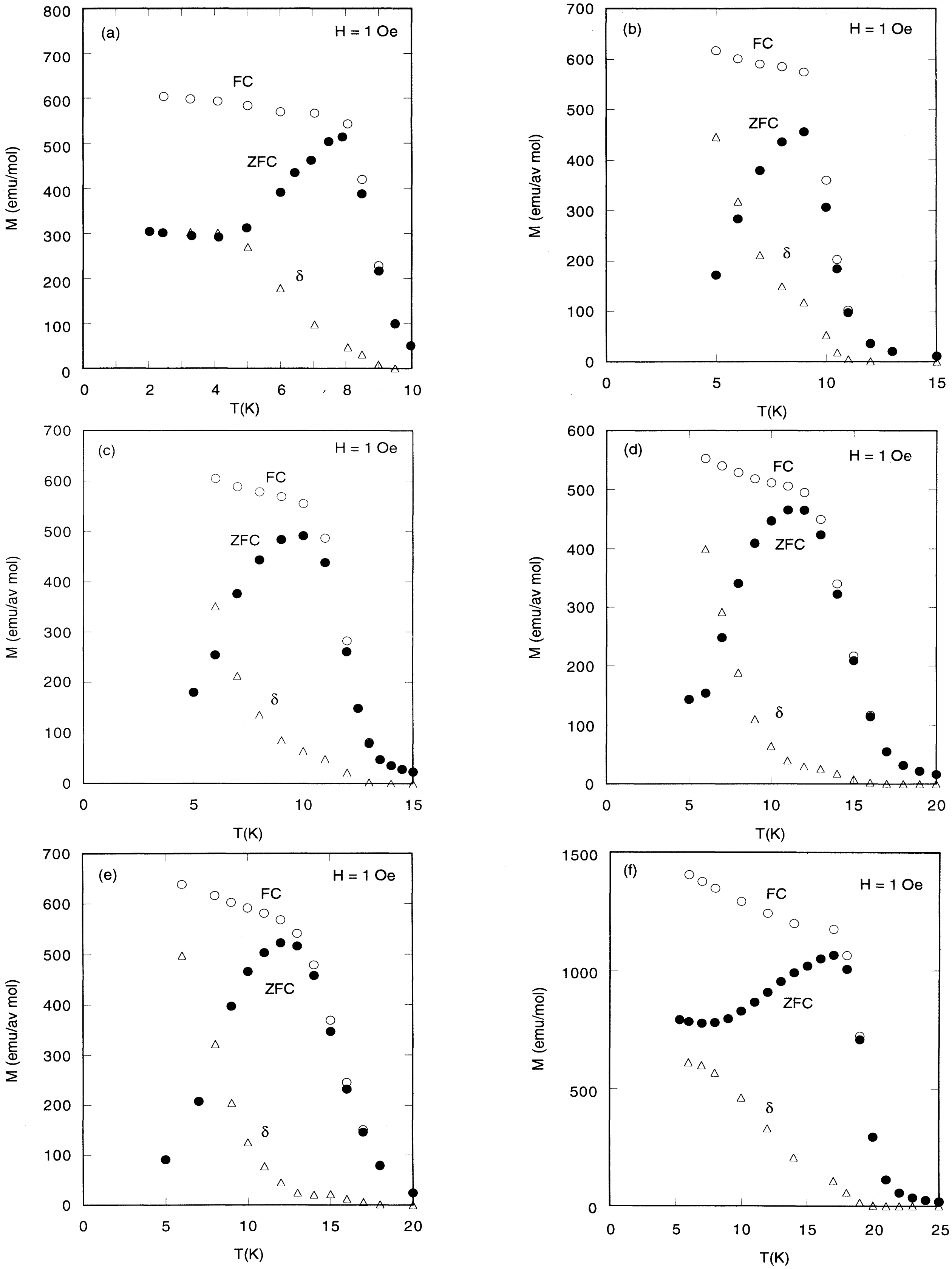

FIG. 3. Temperature variation of M_{FC}(○), M_{ZFC}(●), and $\delta(=M_{FC}-M_{ZFC})$(△) for stage-2 $Co_cNi_{1-c}Cl_2$ GICs. $H=1$ Oe. $H\perp c$. (a) $c=1$, (b) $c=0.65$, (c) $c=0.4$, (d) $c=0.25$, (e) $c=0.1$, and (f) $c=0$.

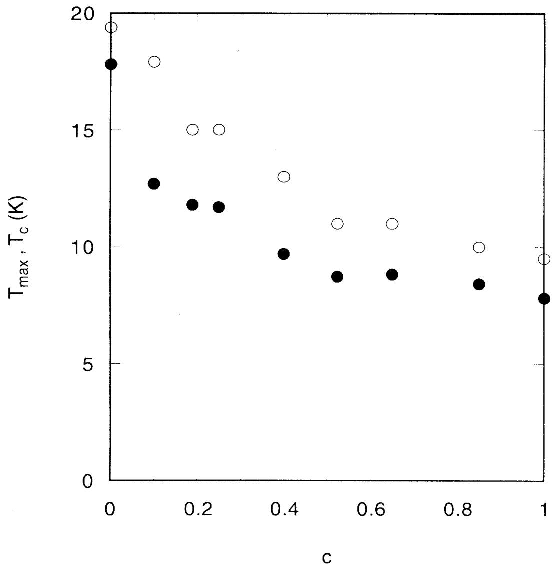

FIG. 4. Concentration dependence of T_c(○) and T_{max}(●) in stage-2 $Co_cNi_{1-c}Cl_2$ GICs.

temperature dependence of M_{ZFC} and M_{FC} for $c=0.9$ is similar to that for $c=1$: (i) the irreversible effect of magnetization appears below T_c ($=17.2$ K), (ii) M_{ZFC} exhibits a broad peak at T_{max} ($=12.6$ K), and (iii) M_{FC} rapidly increases with decreasing temperature below T_c. We also notice that the peak width of M_{ZFC} becomes broader for $0.8 \le c \le 1$ as the Ni concentration decreases, and that this peak disappears for $c=0.75$. The difference δ monotonically increases with decreasing temperature for $0.7 \le c \le 1$ and reduces to zero at any temperature for $c \le 0.65$. These results imply that δ does not show any anomaly around T_{max} for $0.8 \le c \le 1$ and that the irreversible effect disappears for $c \le 0.65$. Figure 6 shows the Ni concentration dependence of T_{max} and T_c for the stage-2 $Ni_cMn_{1-c}Cl_2$ GICs which are derived from the temperature variation of M_{ZFC} and M_{FC}, respectively. Both T_{max} and T_c rapidly decrease with the dilution of Mn^{2+} ions, implying that Mn^{2+} ions behave like a nonmagnetic impurity. The ratio ρ ($=T_c/T_{max}$) rapidly increases with decreasing Ni concentration for $0.8 \le c \le 1$: $\rho=1.09$ at $c=1$, $\rho=1.37$ at $c=0.9$, and $\rho=1.63$ at $c=0.8$. The magnetic phase diagram of T_c vs c agrees with that obtained from the dc magnetic susceptibility measurements.[4]

We have measured the temperature dependence of M_{ZFC} and M_{FC} in stage-2 $Co_cMn_{1-c}Cl_2$ GICs with $c=1$, 0.9, 0.85, 0.8, 0.7, and 0.6. Typical examples of temperature variation in M_{ZFC}, M_{FC}, and δ for stage-2 $Co_cMn_{1-c}Cl_2$ GICs are shown in Fig. 7. The temperature dependence of M_{ZFC}, M_{FC}, and δ for $c=0.9$ is characterized as follows. (i) M_{ZFC} exhibits a broad peak at T_{max} ($=7$ K) and slightly increases with decreasing temperature below 4 K, and (ii) M_{FC} rapidly increases as the temperature decreases below T_c ($=7.8$ K) and almost saturates at 4 K, and (iii) δ does not show any anomaly at T_{max} but has a broad peak at 4 K. We notice that for $0.8 \le c \le 1$ the irreversible effect of magnetization appears below T_c. The broad peak of M_{ZFC} observed for $c=0.9$ changes into a shoulder for $0.8 \le c \le 0.85$. The difference δ for $0.8 \le c \le 0.85$ monotonically increases with decreasing temperature below T_c and shows a broad peak around 5 K. The difference δ for $0.6 \le c \le 0.7$ is almost equal to zero in the temperature range between 2 and 10 K, indicating that the irreversible effect of magnetization disappears. The value of T_c for $0.8 \le c \le 1$ is derived from the temperature variation of δ: $T_c=7.8$ K for $c=0.9$, $T_c=7.0$ K for $c=0.85$, and $T_c=6.5$ K for $c=0.8$.

V. DISCUSSION

Our SQUID magnetization data indicate that our samples can be classified into three types depending on the temperature dependence of M_{ZFC} and M_{FC}. For the Type I compounds such as stage-2 $Co_cNi_{1-c}Cl_2$ GICs ($0 \le c \le 1$), stage-2 $Ni_cMn_{1-c}Cl_2$ GICs ($0.8 \le c \le 1$) and stage-2 $Co_cMn_{1-c}Cl_2$ GICs ($0.9 \le c \le 1$), the ferromagnetic intraplanar exchange interactions are dominant compared to the antiferromagnetic intraplanar exchange interactions. This dominance of ferromagnetic interactions is supported by the fact that the value of M_{FC} for the type I compounds takes a relatively large value at 6 K: for example, $M_{FC}=250-1400$ emu/av mol at 6 K for stage-2 $Ni_cMn_{1-c}Cl_2$ GICs ($0.8 \le c \le 1$). Here we note that M_{FC} is a thermal equilibrium magnetization in the presence of magnetic field and is considered to be a measure for the average magnetization over islands. The temperature dependence of M_{ZFC} and M_{FC} for the type I compounds is characterized as follows. (i) M_{ZFC} shows a broad peak at T_{max} and (ii) δ does not show any anomaly at T_{max} and reduces to zero at T_c ($>T_{max}$). The latter result indicates that these systems undergo a magnetic phase transition only at T_c. Our model for the magnetic phase transition is different from that derived by Wiesler, Suzuki, and Zabel[10] from the magnetic neutron scattering studies on stage-2 $CoCl_2$ GIC and stage-2 $NiCl_2$ GIC. They have claimed that these systems undergo two magnetic phase transitions at T_{cu} and T_{cl} ($<T_{cu}$): $T_{cl}=8.0$ K and $T_{cu}=9.1$ K for stage-2 $CoCl_2$ GIC, and $T_{cl}=17.5$ K and $T_{cu}=22.0$ K for stage-2 $NiCl_2$ GIC. Below T_{cu} a 2D ferromagnetic spin order is established within each island. Below T_{cl} a 3D antiferromagnetic phase occurs through the interplanar antiferromagnetic exchange interaction. The 2D ferromagnetic layers are antiferromagnetically stacked along the c axis. The value of T_{cu} for stage-2 $CoCl_2$ GIC and stage-2 $NiCl_2$ GIC seems to agree with that of T_c determined from the temperature dependence of δ: $T_c=9.5$ K for stage-2 $CoCl_2$ GIC and $T_c=19.4$ K for stage-2 $NiCl_2$ GIC.

The magnetic phase transition of the type I compounds may be understood as follows. Below T_c spins within each island are ferromagnetically aligned, forming a ferromagnetic cluster. The spin directions of ferromagnetic clusters are frozen because of frustrated interisland interactions such as dipole-dipole interaction between ferromagnetic clusters, and interplanar antiferromagnetic

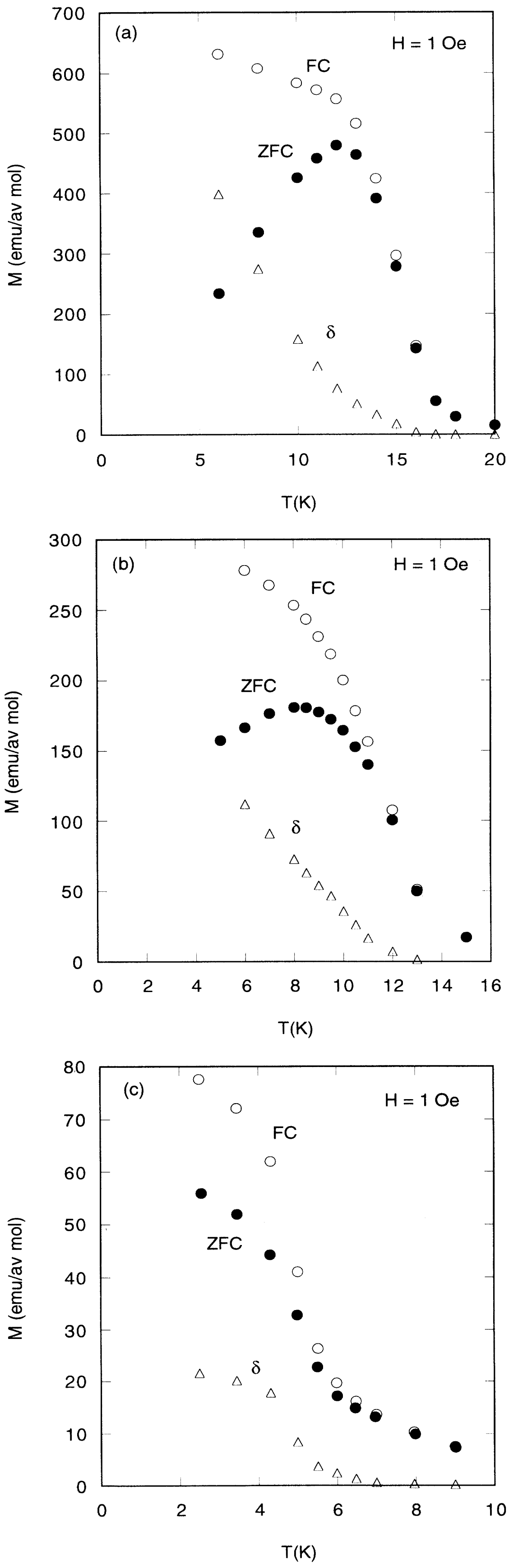

interaction between different layers. The effect of frustrated interisland interaction is not taken into account in the model of Wiesler, Suzuki, and Zabel.[10] We will discuss the origin of frustrated interisland interaction later. The irreversible effect of magnetization is one of the main features for the cluster glass phase. A ferromagnetic cluster in the cluster glass phase behaves like a spin in the spin glass phase. The free energy of the cluster glass phase has a many-valley structure with very many stable states. The zero-field cooling of the system down to low temperature causes the system to fall into one of these valleys. The magnetization M_{ZFC} is different for different valleys. We note that the characteristic temperature variation of M_{ZFC} and M_{FC} observed in our systems is not unique. Similar behaviors are also observed in the 3D Ising random antiferromagnet $Fe_cMn_{1-c}TiO_3$ with $c=0.6$.[13] (i) M_{ZFC} shows two peaks at T_N ($=31.6$ K) and at T_{max} ($=18$ K), (ii) the irreversible effect appears below T_g ($=24.0$ K), and (iii) δ monotonically increases with decreasing temperature and does not show any anomaly at T_{max}. This system is found to undergo two magnetic phase transitions at T_N and T_g. The intermediate phase between T_N and T_g is the antiferromagnetic phase and the low-temperature phase below T_g is the reentrant spin glass (RSG) phase with the coexistence of spin glass phase and antiferromagnetic phase. Ito *et al.*[13] have concluded that the broad peak of M_{ZFC} results from the spin frustration effect in the RSG phase. The cluster glass phase of our system is considered to be one of the RSG phases, because the cluster glass phase has the character of both spin glass phase and ferromagnetic phase. These results may indicate that the appearance of a broad peak in M_{ZFC} is a feature common to the RSG phases.

For the type II compounds such as stage-2 $Ni_cMn_{1-c}Cl_2$ GICs ($0.7 \le c < 0.8$) and stage-2 $Co_cMn_{1-c}Cl_2$ GICs ($0.8 \le c < 0.9$), the antiferromagnetic intraplanar exchange interactions become comparable to the ferromagnetic intraplanar exchange interactions. The replacement of ferromagnetic intraplanar interaction J(Ni-Ni) and J(Co-Co) by antiferromagnetic intraplanar interaction J(Mn-Mn) with the dilution of Mn^{2+} ions gives rise to a drastic decrease in the saturated value of M_{FC}: $M_{FC}=80-200$ emu/av mol at 4 K for stage-2 $Ni_cMn_{1-c}Cl_2$ GICs ($0.7 \le c < 0.8$). We note that this is not the case for the value of M_{FC} at 4 K for stage-2 $Co_cMn_{1-c}Cl_2$ GICs: the value of M_{FC} is still large even for $c=0.8$. The temperature dependence of M_{ZFC} and M_{FC} for the type II compounds is characterized as follows: (i) M_{ZFC} does not show any broad peak, and (ii) δ still appears below T_c. The irreversible effect of magnetization below T_c suggests that the low-temperature phase below T_c may be closely related to a spin-glass-like phase arising from the competition between ferromagnetic and antiferromagnetic interactions within each island. Be-

FIG. 5. Temperature variation of M_{FC}(○), M_{ZFC}(●), and δ ($=M_{FC}-M_{ZFC}$)(△) for stage-2 $Ni_cMn_{1-c}Cl_2$ GICs. $H=1$ Oe $H \perp c$. (a) $c=0.9$, (b) $c=0.8$, and (c) $c=0.7$.

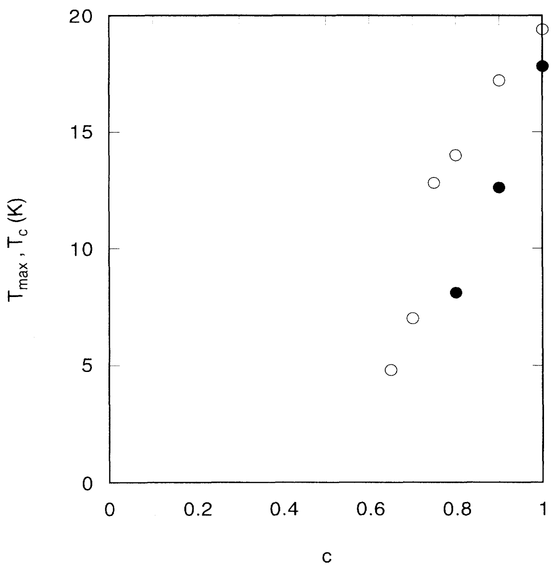

FIG. 6. Concentration dependence of T_c(○) and T_{max}(●) in stage-2 $Ni_cMn_{1-c}Cl_2$ GICs.

cause of the frustrated nature of competing interactions the directions of spins within each island may be frozen. The frustrated interisland interaction is roughly proportional to M_{FC}. As a result of drastic decrease in M_{FC}, the interisland interactions of type II compounds may be much weaker than those of type I compounds, and does not contribute to the long-range spin ordering between islands. For the type III compounds such as stage-2 $Ni_cMn_{1-c}Cl_2$ GICs ($0.6 \le c < 0.7$) and stage-2 $Co_cMn_{1-c}Cl_2$ GICs ($0.6 \le c < 0.8$), the antiferromagnetic intraplanar exchange interactions are dominant compared to the ferromagnetic intraplanar exchange interactions, which leads to a rapid decrease of M_{FC}: for example, $M_{FC}=8$ emu/av mol at 4 K for stage-2 $Ni_cMn_{1-c}Cl_2$ GIC with $c=0.6$ and $M_{FC}=80$ emu/av mol at 4 K for stage-2 $Co_cMn_{1-c}Cl_2$ GIC with $c=0.6$. The temperature dependence of M_{ZFC} and M_{FC} of type III compounds is characterized as follows. (i) M_{ZFC} coincides with M_{FC} at any temperature, and (ii) M_{FC} monotonically decreases with decreasing temperature. This disappearance of irreversible effect implies that no spin frustration effect occurs in these compounds.

It is concluded from the above results that each island at low temperatures is in the ferromagnetic phase, spin-glass phase, and paramagnetic phase depending on the concentration. For stage-2 $Co_cMn_{1-c}Cl_2$ GICs, for example, (i) spins of each island ferromagnetically order, forming a ferromagnetic cluster for $c \ge 0.9$, (ii) they form a spin-glass-like phase with frozen directions of spins for $0.8 \le c < 0.9$, and (iii) they are in the paramagnetic phase for $c < 0.8$. Ozeki and Nishimori[14] have studied the phase diagram of a 2D asymmetric $\pm J$ Ising model on the square lattice by the numerical transfer matrix method. In this model the exchange interaction J_{ij} is only in the nearest-neighbor bonds and is randomly distributed at each bond with the probability weight c of ferromagnetic bonds ($J_{ij}=J$) and $(1-c)$ the probability weight of antiferromagnetic bonds ($J_{ij}=-J$). The c-T phase diagram consists of a ferromagnetic phase for $c > c_u$ (≈ 0.89) and a spin-glass phase for $c_l < c < c_u$ ($c_l \approx 0.8$), and a paramagnetic phase for $c < c_l$. The boundary between the ferromagnetic phase and the spin-glass phase is perpendicular to the concentration axis below the ferromagnetic critical line denoted as Nishimori line,[14] implying the absence of a reentrant transition from the ferromagnetic phase to the spin-glass phase. Thus various kinds of spin order occurring within islands in magnetic RMGICs can be qualitatively explained by the theory of 2D asymmetric $\pm J$ Ising model.

Here we give a brief discussion of the frustrated interisland interactions such as (i) the dipole-dipole interaction in the same intercalate layer and (ii) the interplanar antiferromagnetic interaction between different intercalate layers. Below T_c spins within each island form a ferromagnetic cluster. The diameter of these ferromagnetic clusters R (≈ 500 Å) is much larger than a typical size of superparamagnet (≈ 80 Å).[15] First we consider a dipole-dipole interaction between these ferromagnetic clusters within the same intercalate layer, which may be roughly described by

$$H_d=\frac{1}{R_{ij}^3}\left[\mathbf{M}_i\cdot\mathbf{M}_j-\frac{3(\mathbf{M}_i\cdot\mathbf{R}_{ij})(\mathbf{M}_j\cdot\mathbf{R}_{ij})}{R_{ij}^2}\right], \tag{1}$$

where $\mathbf{M}_i$ and $\mathbf{M}_j$ are the magnetization of ith and jth ferromagnetic clusters, respectively, and $\mathbf{R}_{ij}$ is the vector connecting centers of two clusters. This dipole-dipole interaction may lead to a spin frustration effect which arises from the competition between ferromagnetic and antiferromagnetic interactions. This dipole-dipole interaction favors an antiferromagnetic alignment when both $\mathbf{M}_i$ and $\mathbf{M}_j$ are perpendicular to the direction of the vector $\mathbf{R}_{ij}$, and favors a ferromagnetic alignment when both $\mathbf{M}_i$ and $\mathbf{M}_j$ are parallel to the direction of the vector $\mathbf{R}_{ij}$, respectively. The randomness in the directions of $\mathbf{M}_i$, $\mathbf{M}_j$, and $\mathbf{R}_{ij}$ causes the dipole-dipole interaction to be a frustrated interisland interaction. The number of magnetic ions in each island having a diameter R is given by $N=\pi R^2/(2\sqrt{3}a^2)$, where a is the lattice constant of the triangular lattice ($a=3.55$ Å for stage-2 $CoCl_2$ GIC) and the nearest-neighbor distance between islands is assumed to be equal to R. Then the dipole-dipole interaction between adjacent islands is approximately given by

$$E_d^{AF}=\frac{N^2g^2\mu_B^2S^2}{R^3}=\frac{\pi^2g^2\mu_B^2S^2R}{12a^4}, \tag{2}$$

for the antiferromagnetic alignment ($\mathbf{M}_i=-\mathbf{M}_j$), and is given by $E_d^F=-2E_d^{AF}$ for the ferromagnetic alignment ($\mathbf{M}_i=\mathbf{M}_j$), respectively. The dipole-dipole interaction energy is proportional to the diameter R and may contribute to a frustrated interisland interaction when R becomes large enough.

Next we consider an interplanar antiferromagnetic exchange interaction between ferromagnetic clusters in different intercalate layers. The effective interplanar exchange interaction may be described by[16]

$$J'_{\text{eff}} \approx J'S(S+1)p\frac{\pi R^2}{2\sqrt{3}a^2}\ , \tag{3}$$

where p is the degree of the overlapping of one ferromagnetic cluster with diameter R in an intercalate layer on the other island with the same radius in the nearest-neighbor adjacent intercalate layers. The value of p depends on the position of islands within each intercalate layer ($0<p<1$). Because of random distribution of islands inside each intercalate layer the value of p may be assumed to be equal to $\frac{1}{2}$. This effective interplanar interaction favors an antiferromagnetic alignment for ferromagnetic clusters in the different intercalate layers. The value of $|J'_{\text{eff}}|$ is proportional to the square of R. Here we define the diameter R_0 by

$$R_0=\frac{\sqrt{3}}{6pa^2}\frac{g^2\mu_B^2 S}{|J|(S+1)}\left|\frac{J}{J'}\right|\ , \tag{4}$$

where the effective interplanar exchange interaction ($|J'_{\text{eff}}|$) is on the same order as that of the dipole-dipole interaction ($|E_d^{AF}|$). The value of R_0 is estimated as $R_0 \approx 0.2|J/J'| \approx 2000/\lambda$ Å for the state-2 $CoCl_2$ GIC where $J=7.75$ K, $S=\frac{1}{2}$, $g=6.4$, and $a=3.55$ Å. The ratio $|J'/J|$ is assumed to be given by $\lambda\times10^{-4}$ ($0<\lambda<10$). When R is much larger than R_0, the effective interplanar interaction dominantly contributes to the frustrated interisland interaction. When R is much smaller than R_0, the dipole-dipole interaction dominantly contributes to the frustrated interisland interaction. The

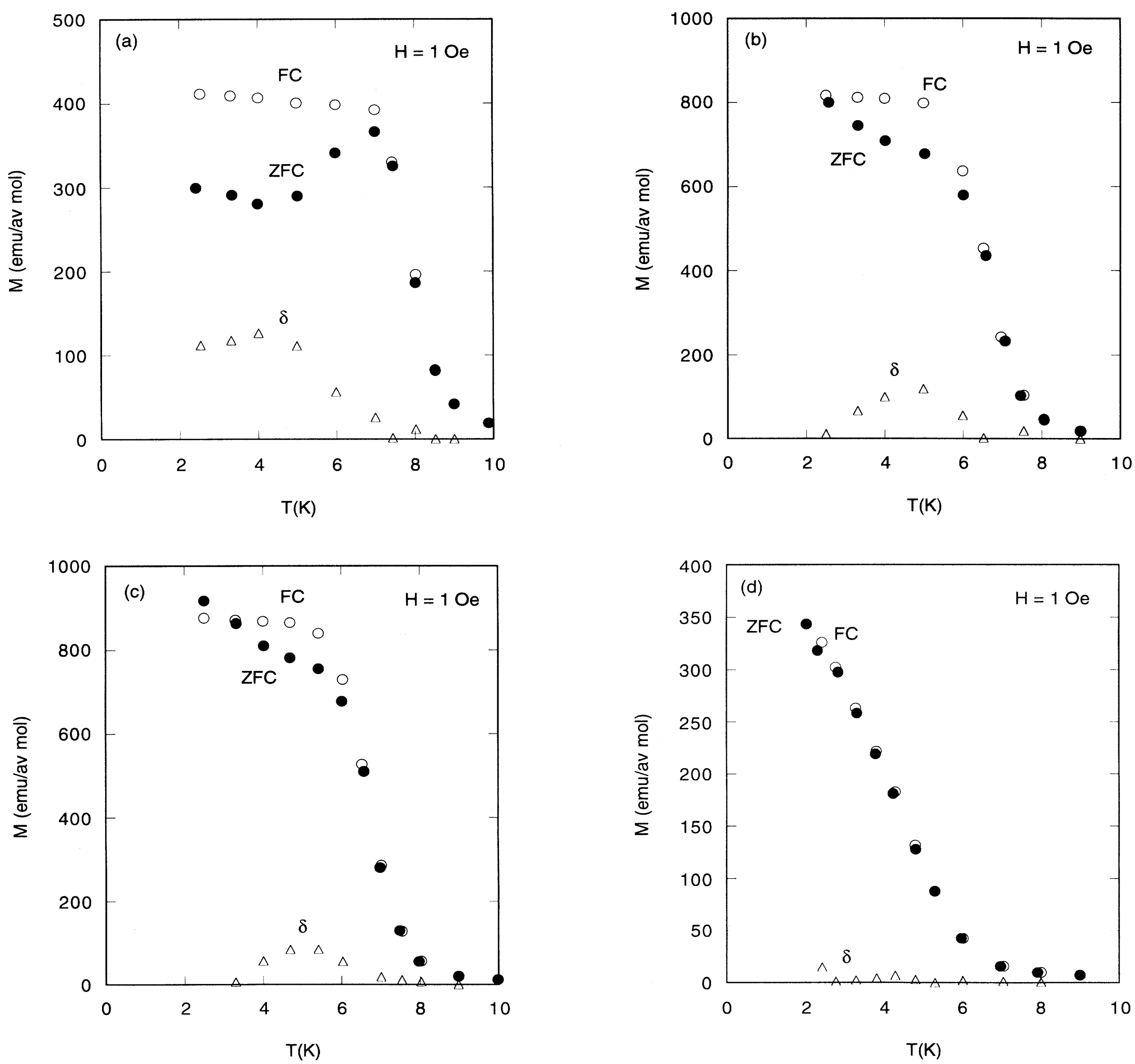

FIG. 7. Temperature variation of M_{FC}(○), M_{ZFC}(●), and δ ($=M_{\text{FC}}-M_{\text{ZFC}}$)(△) for stage-2 $Co_cMn_{1-c}Cl_2$ GICs. $H=1$ Oe. $H\perp c$. (a) $c=0.9$, (b) $c=0.85$, (c) $c=0.8$, and (d) $c=0.7$.

value of R_0 is estimated to be on order of the diameter of islands (≈ 500 Å) for $\lambda=4$. This implies that both the dipole-dipole interaction and the effective interplanar interaction contribute to the frustrated interisland interaction.

Finally we discuss the origin of the broad peak in M_{ZFC} at T_{max}. Below T_{max} the spin directions of ferromagnetic clusters are frozen because of the frustrated interisland interaction. The thermal energy ($k_B T$) increases with increasing temperature, and becomes comparable with the frustrated interisland interaction around T_{max}. Then T_{max} may be approximated by

$$T_{max} \approx \frac{g^2 S^2 R}{a^4} \left[\frac{M}{M_s} \right]^2 [K] , \tag{5}$$

where R and a are in units of Å, M_s is the saturation magnetization and the ratio M/M_s is the degree of ferromagnetic spin ordering within each island. The value of T_{max} can be estimated as $T_{max}=0.064R(M/M_s)^2[K]$ for the stage-2 $CoCl_2$ GIC: $T_{max} \approx 8$ K when we set $R=500$ Å and $M/M_s=\frac{1}{2}$. This value of T_{max} is on the same order as that of T_{max} which is experimentally obtained.

VI. CONCLUSION

We have discussed the magnetic phase transition of magnetic RMGICs. For the type I compounds where the intraplanar ferromagnetic interactions are dominant, a cluster glass phase appears below T_c. The spin directions of ferromagnetic clusters are frozen because of the frustrated interisland interaction consisting of the combination of dipole-dipole interaction and interplanar antiferromagnetic interaction. The thermal energy increases as temperature increases. When the temperature is close to T_{max}, the thermal energy becomes comparable to the magnitude of the frustrated interisland interaction. Just above T_{max} the spin directions of ferromagnetic clusters become random. The spins in the ferromagnetic clusters are still coupled through the ferromagnetic intraplanar exchange interaction. With further increasing temperature, the spins within each island begin to fluctuate because of thermal energy. Above T_c the spin direction in islands becomes disordered.

Due to frustrated interisland interactions, the mechanism of magnetic phase transition in the type I compounds is much more complicated than we previously thought. For further understanding of this mechanism, it is necessary to do magnetic neutron scattering studies of these compounds in the ZFC and FC states.

ACKNOWLEDGMENTS

The SQUID magnetization and electron microprobe measurements were carried out when two of us (I.S.S. and M.S.) stayed at the Institute for Molecular Science in Japan as visiting scientists. We are grateful to H. Ogata, Y. Nakazawa, and K. Kato for their help on the SQUID magnetization measurement and T. Terui and M. Sakai for their help on the electron microprobe measurement. We would like to thank H. Suematsu for providing us with high-quality single-crystal kish graphites, and F. Khemai, J. Morillo, M. Yeh, and L. F. Tien for their help with sample preparation of RMGICs. We would also like to thank to C. R. Burr for his critical reading of this manuscript. The work at SUNY at Binghamton was supported by National Science Foundation Grant No. DMR-8902351 and DMR-9201656, and the work at the Institute for Molecular Science was supported by Grant-in-Aid for Scientific Research from the Ministry of Education, Science, and Culture of Japan 04NP0301.

[1] M. Yeh, M. Suzuki, and C. R. Burr, Phys. Rev. B **40**, 1422 (1989).

[2] M. Yeh, I. S. Suzuki, M. Suzuki, and C. R. Burr, J. Phys. Condensed Matter **2**, 9821 (1990).

[3] M. Suzuki, I. S. Suzuki, W. Zhang, and C. R. Burr, Phys. Rev. B **46**, 5311 (1992).

[4] I. S. Suzuki, F. Khemai, M. Suzuki, and C. R. Burr, Phys. Rev. B **45**, 4721 (1992).

[5] I. S. Suzuki, M. Suzuki, L. F. Tien, and C. R. Burr, Phys. Rev. B **43**, 6393 (1991).

[6] I. S. Suzuki and M. Suzuki, J. Phys. Condensed Matter **3**, 8825 (1991).

[7] J. T. Nicholls and G. Dresselhaus, Phys. Rev. B **41**, 9744 (1990).

[8] I. S. Suzuki, C. J. Hsieh, F. Khemai, C. R. Burr, and M. Suzuki, Phys. Rev. B **47**, 845 (1993).

[9] D. G. Wiesler, M. Suzuki, P. C. Chow, and H. Zabel, Phys. Rev. B **34**, 7951 (1986).

[10] D. G. Wiesler, M. Suzuki, and H. Zabel, Phys. Rev. B **36**, 7051 (1987).

[11] M. Suzuki, *Critical Reviews in Solid State and Materials Science* (CRC, Boca Raton, FL, 1990), Vol. 16, p. 237.

[12] G. Dresselhaus, J. T. Nicholls, and M. S. Dresselhaus, in *Graphite Intercalation Compounds II,* edited by H. Zabel and S. A. Solin (Springer-Verlag, Berlin, 1992), p. 247.

[13] A. Ito, H. Aruga, M. Kikuchi, Y. Synono, and H. Takei, Solid State Commun. **66**, 475 (1988).

[14] Y. Ozeki and H. Nishimori, J. Phys. Soc. Jpn. **56**, 3265 (1987).

[15] D. G. Rancourt, J. Magn. Magn. Mater. **51**, 133 (1985).

[16] M. Matsuura and H. Zabel, J. Magn. Magn. Mater. **90&91**, 260 (1990).